Modeling of sawtooth destabilization during radiofrequency heating experiments in tokamak plasmas

K. G. McClements, R. O. Dendy, R. J. Hastie, and T. J. Martin

Citation: Phys. Plasmas 3, 2994 (1996); doi: 10.1063/1.871629
View online: http://dx.doi.org/10.1063/1.871629
View Table of Contents: http://pop.aip.org/resource/1/PHPAEN/v3/i8
Published by the American Institute of Physics.

Modeling of sawtooth destabilization during radio-frequency heating experiments in tokamak plasmas

K. G. McClements, R. O. Dendy, R. J. Hastie, and T. J. Martin
UKAEA, Fusion (UKAEA/Euratom Fusion Association), Culham, Abingdon, Oxfordshire, OX14 3DB, United Kingdom

(Received 23 January 1996; accepted 6 May 1996)

Sawtooth oscillations in tokamaks have been stabilized using ion cyclotron resonance heating (ICRH), but often reappear while ICRH continues. It is shown that the reappearance of sawteeth during one particular ICRH discharge in the Joint European Torus (JET) [Campbell *et al.*, Phys. Rev. Lett. **60**, 2148 (1988)] was correlated with a change of sign in the energy δW associated with $m=1$ internal kink displacements. To compute δW, a new analytical model is used for the distribution function of heated minority ions, which is consistent with Fokker–Planck simulations of ICRH. Minority ions have a stabilizing influence, arising from third adiabatic invariant conservation, but also contribute to a destabilizing shift of magnetic flux surfaces. As the minor radius of the $q=1$ surface rises, the stabilizing influence of minority ions diminishes, and the shape of the plasma cross section becomes increasingly important. It is shown that an increase in ICRH power can destabilize the kink mode: this is consistent with observations of sawteeth in JET discharges with varying levels of ICRH. It is suggested that the sawtooth-free period could be prolonged by minimizing the vertical extent of the ICRH power deposition profile. [S1070-664X(96)02308-7]

I. INTRODUCTION

Sawtooth-like oscillations in the soft x-ray emission from a tokamak plasma were first reported by von Goeler and co-workers in 1974.[1] Although such oscillations may have the beneficial effect of removing high-Z impurities, their suppression is generally regarded as desirable, from the point of view of optimizing plasma performance. It has been known for several years that sawtooth stabilization can be achieved for a limited period of time using the heating properties of electromagnetic waves in the ion cyclotron range of frequencies (ICRF).[2,3] Since ICRF waves are frequently used to provide auxiliary heating in large tokamaks, it is important to understand as fully as possible the mechanism whereby such waves can bring about sawtooth stabilization.

ICRF heating experiments that brought about sawtooth stabilization in the Joint European Torus (JET) tokamak are described in Ref. 2; similar experiments in the Tokamak Fusion Test Reactor (TFTR) are reported in Ref. 3. In the case of JET, the majority and minority ions were, respectively, deuterons and protons.[4] In one JET discharge (hereinafter referred to as discharge A), the central electron temperature T_{e0} initially exhibited normal sawtoothing behavior, but rose to an essentially steady value of around 6.4 keV shortly after the onset of ion cyclotron resonance heating (ICRH). This steady state persisted for approximately 1 s, during which there was an almost complete absence of magnetohydrodynamic (MHD) activity. A sawtooth collapse in T_{e0} then followed, triggered apparently by an instability with toroidal and poloidal mode numbers $n=1$, $m=1$. The sawtooth occurring at the end of the stable period had an inversion radius r_i of around 50–60 cm, whereas the inversion radius during the initial sawtoothing phase (prior to the onset of ICRH) was around 40 cm. Throughout the stable period, the safety factor q in the plasma center was below unity.

In a second JET discharge described in Ref. 2 (hereinafter discharge B), sawtooth stabilization did not occur: T_{e0} rose sharply at the onset of ICRH, but continued to exhibit sawtooth behavior. In both discharges A and B, the plasma current I_p was 2.2 MA, and the safety factor at the plasma edge q_a was equal to 5.2. The most significant difference between the two experiments was in the ICRF power level: around 4.3 MW in discharge A, and around 6 MW in discharge B. Since stabilization in discharge A was evidently brought about by ICRH, one might expect an increase in ICRH power to give greater stability: in the 4–6 MW range, the opposite was the case. A similar phenomenon has been observed in TFTR (see Fig. 4 in Ref. 3).

The fact that an $m=n=1$ instability triggered the end of the stable period in discharge A strongly implies that the potential energy δW associated with $m=1$ internal kink displacements plays a crucial role in determining whether or not sawteeth occur: in the ideal limit, $\delta W<0$ is a necessary and sufficient condition for instability. In a thermally relaxed plasma, δW can be computed using ideal MHD.[5] However, trapped ICRF-heated minority ions give rise to an additional kinetic term in δW, which is generally positive and thus stabilizing.[6] In order to compute this term, it is necessary to specify the distribution function of minority ions: in Ref. 6, the present authors used a model distribution that is appropriate for the case of ICRH experiments in JET to obtain a complicated but numerically tractable integral expression for the trapped minority ion contribution to δW. The parameters appearing in this expression are clearly defined experimental quantities, such as ICRF power and the height of the power deposition profile.

The main aim of this paper is to compute δW for ICRF-heated JET discharges in a fully self-consistent way, taking into account both anisotropic pressure and kinetic effects, and using parameters that correspond as closely as possible

 1070-664X/96/3(8)/2994/10/$10.00

to discharges A and B discussed in Ref. 2. To achieve this, it is necessary to calculate the kinetic contribution to δW using a realistic representation of the heated ion distribution, and to extend the Bussac toroidal energy principle[5] to the case of anisotropic plasma pressure with shaping, using the analyses of Edery and co-workers,[7] Mikhailovskii,[8] and Madden and Hastie.[9] For the purpose of comparing theory with experiment, it is also necessary to focus on the uncertainties affecting quantities such as minority ion concentration and ICRF power deposition profiles, which determine the values of parameters that are central to the theory. A crucial test of the complete model is, then, that the computed values of δW are positive during the sawtooth-free period of discharge A, and close to zero or negative at the end of that period, within the limits of experimental uncertainty.

Several other authors have examined the effect of ICRF waves on sawtooth oscillations. Porcelli and co-workers[10] compared predictions of a model developed by Pegoraro and co-workers[11,12] with data from various ICRF-heated JET discharges in which sawtooth suppression was observed. In this model, the kinetic term in δW was evaluated numerically, using a model of the minority ion distribution that reflects the anisotropy of ICRF heating. The only parameters of the heated ion distribution that can be measured directly are global ones, such as total energy content, and for this reason it was necessary for Porcelli and co-workers to make simplifying assumptions about the spatial profiles of heated ions. Also, the model presented in Refs. 11 and 12 assumes an ordering in which the MHD contribution to δW can be described by a scalar plasma pressure. Such an ordering was also assumed by Cheng,[13] in a wide-ranging study of energetic particle effects on MHD instabilities; by Phillips and co-workers,[3] in the context of sawtooth stabilization in TFTR; and by Zabiégo and co-workers,[14] who used their analysis to interpret sawtooth stabilization experiments in the Tore Supra tokamak. Porcelli and co-workers[15] have argued that the finite widths of ICRF-heated ion orbits tend to inhibit stabilization at high ICRF power, while Bhatnagar and co-workers[16] have demonstrated experimentally that enhanced sawtooth stability can be achieved by modifying the plasma current profile to reduce magnetic shear at the surface defined by $q=1$.

In a real tokamak plasma, with finite electrical resistivity, instability can occur when δW is positive, although the exact location of the stability boundary in this case is not clear. White and co-workers[17,18] have carried out stability analyses of the resistive and ideal internal kink modes, taking into account the presence of a trapped ICRF-heated ion population with a unique pitch angle. Recently, it has been suggested by Levinton and co-workers[19] that δW may have been strongly negative during some sawtooth-free discharges in TFTR. Auxiliary heating in these discharges was provided by neutral beam injection. Levinton and co-workers assumed isotropic plasma pressure, and used ideal MHD to compute δW: they assumed that the kinetic contribution to δW could be neglected, on the grounds that the neutral beams were injected tangentially to the magnetic axis and consequently supplied few trapped ions to the plasma. Sawtooth suppression in TFTR has instead been attributed to the fact that the saturation amplitude of the $m=1$ kink mode may be very low, because of two-fluid effects involving the electron and ion diamagnetic frequencies.[20] There appears to be strong evidence, however, that the total δW (including the kinetic contribution of energetic ions) plays a significant role in determining the stability of sawtooth oscillations in ICRF-heated JET discharges (see, e.g., Ref. 10).

As a preamble to our principal objective, that of computing δW using a fully self-consistent set of parameters (Sec. III), we first show quantitatively that the model distribution proposed in Ref. 6 is a realistic representation of an ion population heated by ICRH (Sec. II). After a brief discussion of resistive and finite ion Larmor radius effects, we conclude by examining possible experimental strategies for prolonging sawtooth-free periods in future ICRH experiments.

II. ICRF-HEATED MINORITY ION DISTRIBUTION

For the purposes of the present discussion, the model distribution proposed in Ref. 6 can most usefully be written in the form

$$F_h(\mu,\mathscr{E},r)=2n_h(r)\left(\frac{m_h}{2\pi T_\perp(r)}\right)^{3/2}G(r)\times\exp\left[-m_h\left(\frac{\mu B_0}{T_\perp(r)}+\frac{|\mathscr{E}-\mu B_0|}{T_\parallel(r)}\right)\right], \quad (1)$$

where the magnetic moment μ and energy $\mathscr{E}$ are both normalized to the minority ion mass m_h; B_0 is the magnetic induction at $R=R_0$, where R is distance from the axis of symmetry and R_0 is the major radius; $G(r)$ is a normalization factor that is computed in the Appendix of Ref. 6; n_h is the minority ion density; r is a minor radial coordinate; and $T_\parallel$, $T_\perp$ are parameters whose values are determined by a model of ICRF heating that was proposed by Stix.[21] We have assumed that, on a given flux surface, maximum power deposition occurs at $R=R_0$, where $\mu B_0=v_\perp^2/2$ and $|\mathscr{E}-\mu B_0|=v_\parallel^2/2$ ($v_\perp$ and $v_\parallel$ denoting velocity components perpendicular and parallel to the magnetic field). At $R=R_0$, the function F_h is thus bi-Maxwellian, with perpendicular and parallel temperatures $T_\perp, T_\parallel$: the nature of the heating process is such that $T_\perp$ is normally larger than $T_\parallel$. At $R\neq R_0$, F_h is not bi-Maxwellian. One can demonstrate this by determining the locus of points in $(v_\parallel, v_\perp)$ space corresponding to constant F_h. At $R=R_0$, each locus of constant F_h is an ellipse; if the magnetic induction is of the form $B(r,\theta)=B_0(1-\epsilon\cos\theta)$, where θ is the poloidal angle and $\epsilon\equiv r/R_0$ is the local inverse aspect ratio, the locus at $R\neq R_0$ is defined by the equation

$$\frac{v_\perp^2}{1-\epsilon\cos\theta}+\frac{T_\perp}{T_\parallel}\left|v_\perp^2+v_\parallel^2-\frac{v_\perp^2}{(1-\epsilon\cos\theta)}\right|=u^2, \quad (2)$$

where u is a constant. Setting $\theta=0$ (corresponding to the midplane, outboard of the magnetic axis), and assuming $v_\perp^2<v_\parallel^2(1/\epsilon-1)$, we obtain

$$v_\parallel^2=\left(\frac{T_\parallel}{T_\perp}\right)\frac{u^2-v_\perp^2[1-(T_\perp/T_\parallel)\epsilon]}{1-\epsilon}. \quad (3)$$

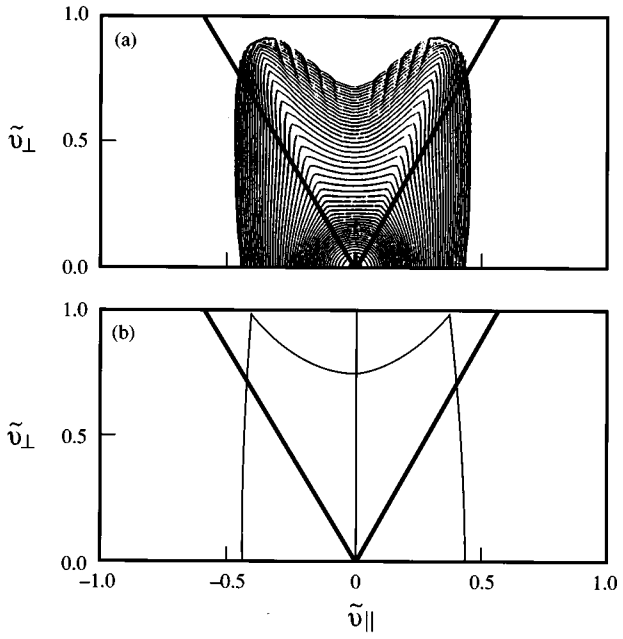

FIG. 1. ICRF-heated ion distribution function contours in midplane velocity–space coordinates $(\tilde{v}_\parallel, \tilde{v}_\perp)$. (a) Deuterium distribution in a 50:50 deuterium–tritium plasma, obtained by solving numerically a steady-state Fokker–Planck equation.[22] The local inverse aspect ratio ϵ is 0.14. (b) Contour of the function F_h, corresponding to parameters $\epsilon=0.14$, $T_\parallel/T_\perp=0.17$. The velocity components are normalized to the speed of a 1.2 MeV deuteron. In both (a) and (b) the trapped–passing boundary is indicated by diagonal lines.

If, on the other hand, $v_\perp^2 > v_\parallel^2(1/\epsilon - 1)$, we have

$$v_\perp^2 = \frac{u^2 + v_\parallel^2 (T_\perp/T_\parallel)(1-\epsilon)}{1+(T_\perp/T_\parallel)\epsilon}. \tag{4}$$

Since $0 \leqslant \epsilon \leqslant 1$, Eq. (4) defines a hyperbola in $(v_\parallel, v_\perp)$ space whose center lies at the origin. Equation (3) defines an ellipse or a hyperbola if $1-(T_\perp/T_\parallel)\epsilon$ is, respectively, positive or negative. In either case, the two conics defined by Eqs. (3) and (4) meet at a pitch angle defined by $\epsilon v_\perp^2 = v_\parallel^2(1-\epsilon)$. It is straightforward to show that this is the pitch angle in the midplane of an ion that undergoes bounce reflection at $\theta = \pm 90°$, i.e. the points of maximum ICRF power deposition on a given flux surface.

We now compare Eqs. (3) and (4) with contours of constant F_h obtained by solving numerically a steady-state Fokker–Planck equation that describes ICRH.[22] Figure 1(a), taken from Ref. 22, depicts the steady-state deuterium distribution in a 50:50 deuterium–tritium plasma. The quantities $\tilde{v}_\parallel$ and $\tilde{v}_\perp$ are midplane velocity components, normalized to the speed of a 1.2 MeV deuteron. The local inverse aspect ratio is 0.14. The trapped–passing boundary, corresponding to bounce reflection at $\theta = \pm 180°$, is indicated by solid diagonal lines. Figure 1(b) shows a single contour of the function F_h defined by Eq. (1), with $\epsilon=0.14$ and $T_\parallel/T_\perp=0.17$. Solid diagonal lines have again been used to represent the trapped–passing boundary. The contour shape is independent of u: the chosen values of u and $T_\parallel/T_\perp$ are such that the contour cuts the $\tilde{v}_\parallel$ and $\tilde{v}_\perp$ axes at the same points as the outermost contour in Fig. 1(a). By adjusting the value of only one free parameter $(T_\parallel/T_\perp)$, we thus obtain a distribution function contour whose shape closely resembles those obtained in a full Fokker–Planck calculation. In particular, the curves in Figs. 1(a) and 1(b) both exhibit sharply defined features at $\epsilon v_\perp^2 = v_\parallel^2(1-\epsilon)$, and local minima at $\tilde{v}_\parallel = 0$. We infer from this that Eq. (1), despite its simplicity, provides a realistic representation of ion distributions heated by ICRF waves.

III. EVALUATION OF KINK ENERGY

We consider a toroidal plasma, undergoing an internal kink displacement with mode numbers $m=1$ and $n=1$. The resulting change in potential energy is

$$\delta W = 6\pi^2 R_0 \xi_0^2 \frac{B_0^2}{\mu_0}\left(\frac{r_1}{R_0}\right)^4 \{\delta\tilde{W}_k + \delta\tilde{W}_T + \delta\tilde{W}_{\text{shape}}\}$$
$$\equiv 6\pi^2 R_0 \xi_0^2 \frac{B_0^2}{\mu_0}\left(\frac{r_1}{R_0}\right)^4 \delta\tilde{W}. \tag{5}$$

Here, ξ_0 is the displacement of the plasma within the $q=1$ surface; r_1 is the minor radial coordinate of that surface; μ_0 is the vacuum permeability (we use SI units throughout); $\delta\tilde{W}_k$ is a kinetic contribution to the kink energy, arising from the presence of trapped ICRF-heated minority ions;[6] $\delta\tilde{W}_T$, evaluated in Refs. 5 and 8, is a quadratic function of the poloidal beta, which, for an isotropic plasma, is defined as

$$\beta_p = -\frac{2\mu_0}{\epsilon_1^2 B_0^2}\int_0^{r_1} \frac{r^2}{r_1^2}\frac{dp}{dr}\,dr, \tag{6}$$

where p is pressure and ϵ_1 is the inverse aspect ratio of the $q=1$ surface; and $\delta\tilde{W}_{\text{shape}}$ arises from departures of the plasma cross section from circularity.[7] The sum $\delta\tilde{W}_T + \delta\tilde{W}_{\text{shape}}$ constitutes the MHD component of the kink energy referred to in the Introduction: $\delta\tilde{W}_T$ is one-third of the dimensionless kink energy defined in Ref. 5. We consider separately the problems of evaluating $\delta\tilde{W}_k$, $\delta\tilde{W}_T$, and $\delta\tilde{W}_{\text{shape}}$.

A. Kinetic hot ion contribution to kink energy

The numerical evaluation of $\delta\tilde{W}_k$, with F_h given by Eq. (1), is greatly facilitated if the kink mode frequency ω is much smaller than the average toroidal precessional drift frequency of the heated ions. We assume that this inequality applies in the case of kink perturbations associated with sawtooth events. In Ref. 6, an integral expression was obtained for a quantity that consisted of $\delta\tilde{W}_k$ plus the contribution of trapped minority ions to the MHD component of δW. In this paper, it is convenient to incorporate the latter into $\delta\tilde{W}_T$, and to compute $\delta\tilde{W}_k$ alone. Expressing F_h as a function of r, $\mathscr{E}$, and $\lambda \equiv v_\perp^2/(v^2 B)$, we have[6]

$$\delta\tilde{W}_k = -\frac{2\sqrt{2}\pi}{3}\frac{\mu_0 m_h}{B_0 R_0}\left(\frac{R_0}{r_1}\right)^4 \int_0^{r_1} r\,dr \int_{1/B_{\min}}^{1/B_{\max}} d\lambda$$
$$\times \int_0^\infty \mathscr{E}^{3/2}\,d\mathscr{E}\,\frac{\partial F_h}{\partial r}\,\frac{I_q^2}{I_c + s I_s}, \tag{7}$$

where $B_{\min}=B_0(1-\epsilon)$, $B_{\max}=B_0(1+\epsilon)$ are the minimum and maximum values of B on a given flux surface, $s\equiv d\ln q/d\ln r$ is magnetic shear, and I_c, I_s, I_q are given by

$$I_c=\int_{-\theta_b}^{\theta_b}\frac{d\theta}{2\pi}\frac{\cos\theta}{(1-\lambda B)^{1/2}}, \tag{8}$$

$$I_s=\int_{-\theta_b}^{\theta_b}\frac{d\theta}{2\pi}\frac{\theta\sin\theta}{(1-\lambda B)^{1/2}}, \tag{9}$$

$$I_q=\int_{-\theta_b}^{\theta_b}\frac{d\theta}{2\pi}\frac{\cos q\theta}{(1-\lambda B)^{1/2}}, \tag{10}$$

the limits of the integrals denoting the poloidal angles at which bounce reflection occurs. These integrals depend on minority ion pitch angle: at a certain trapped pitch angle $I_c+sI_q=0$, which means that $\delta\tilde{W}_k$ has an imaginary part. This reflects a wave–particle resonance between the kink mode and heated ions with bounce-averaged precessional drift frequencies close to ω.

In this paper we are concerned solely with the real part of $\delta\tilde{W}_k$, which is given by the principal part of the λ integral in Eq. (7). A numerically tractable expression for $\mathrm{Re}(\delta\tilde{W}_k)$ may be obtained by following a procedure closely analogous to that used in Ref. 6: only terms that are of leading order in $1-q$ and s are retained, and integration by parts is used to achieve further simplification. The final result, which is similar to Eq. (66) in Ref. 6, can be readily evaluated numerically for any prescribed radial profiles of $T_\perp$, $T_\parallel$, n_h, and q. The first of these, $T_\perp(r)$, is determined by the spatial dependence of ICRF power deposition density, $P_d(r,\theta)$. In Ref. 6 the following representation was used:

$$P_d(r,\theta)=\frac{P_c}{2\pi^2R_0Dd}\exp\left(-\frac{(R-R_0)^2}{d^2}-\frac{Z^2}{D^2}\right), \tag{11}$$

where R,Z, respectively, denote the horizontal distance from the axis of symmetry and vertical distance from the midplane, and P_c, d, D are constants. The coupling of ICRF waves to minority ions is a consequence of cyclotron resonance, and, since B varies more rapidly with R than it does with Z, one expects that in most cases $D>d$. The finite spread of minority ion velocities means that the Doppler resonance condition is satisfied for a range of values of B, and so cyclotron resonance can occur over a finite region of space on either side of $R=R_0$. The width of this region is typically of the order of 0.1 m.[23]

The Stix model[21] predicts that $T_\perp\simeq\rho_{\mathrm{RF}}\tau_S/2n_h$, where ρ_{RF} is the ICRF power density coupled to the minority ions, and τ_S is the Spitzer slowing-down time associated with minority ion–electron collisions. In Ref. 6, ρ_{RF} was identified with $\hat{P}_d(r)$, the peak value of $P_d(r,\theta)$ on a given flux surface. In the case of an ICRH power deposition profile that peaks at $R=R_0$, it can be shown that $\hat{P}_d(r)\propto\exp(-r^2/D^2)$ [see Eq. (38) in Ref. 6]. Putting $\rho_{\mathrm{RF}}=\hat{P}_d$, the Stix formula then becomes

$$T_\perp(r)=\frac{\tau_S(r)P_c}{4\pi^2R_0Ddn_h(r)}\exp\left(-\frac{r^2}{D^2}\right). \tag{12}$$

The slowing-down time is a function of electron density n_e and temperature T_e, with gradient scale lengths of the order of the plasma minor radius a. If the minority ion density varies on a similar length scale, the radial profile of $T_\perp$ will be determined essentially by the value of $D\ll a$. On this basis, an empirical estimate of D can be inferred from observations of neutrons and γ rays produced in reactions between heated minority ions and plasma impurities.[24] Alternatively, one can predict the value of D using ray-tracing and full wave calculations of ICRF power deposition.[25] Both Refs. 24 and 25 deal with the case that is most relevant to the present discussion, namely that of hydrogen minority heating in a JET plasma consisting predominantly of deuterium. The neutron emission profile in Fig. 3 of Ref. 24 has an e-folding width of around 0.5 m, while the computed power deposition profiles in Fig. 1 of Ref. 25 imply a value of D in the range 0.2–0.3 m. The true value of D is thus rather uncertain: we adopt here the lower figure of 0.2 m.

In Eqs. (11) and (12), P_c is the wave power that is absorbed by minority ions: in general, this is less than the total ICRF wave power P_{RF}, a fraction of which is always absorbed by electrons via Landau and transit time damping. If, as in discharges A and B, the wave is in simultaneous cyclotron resonance with more than one ion species, the energy that is absorbed via cyclotron damping will be partitioned among those species. If, for example, the plasma contains a high concentration of fully ionized carbon,[23] there are then three ion species in simultaneous cyclotron resonance with the wave. In those circumstances it is not clear what fractional wave power P_c/P_{RF} is likely to be absorbed by minority ions. It is also difficult to obtain accurate values for the parameters d and n_h. For these reasons, Eq. (12) is of limited use as a formula for estimating $T_\perp$. However, observations of hydrogen atoms formed by charge transfer from hydrogen-like impurity ions to ICRF-heated protons have recently been used as a direct diagnostic of F_h in JET.[26] More specifically, the observations yielded the perpendicular velocity distribution of protons, integrated along a vertical line of sight through the plasma center. The Gaussian variation of $T_\perp$ with r, predicted by Eq. (12), implies that any mean temperature inferred by this method will lie close to $T_\perp(0)$. At low ICRF power ($P_{\mathrm{RF}}\sim$2–4 MW), the line-integrated F_h could be well approximated by a Maxwellian distribution, with $T_\perp$ typically lying in the range 80–140 keV (see Fig. 6 in the first paper of Ref. 26). In these experiments the measured values of $n_e(0)$ and $T_e(0)$ were similar to those of discharge A. We infer from this that 140 keV is a reasonable estimate of $T_\perp(0)$ in discharge A. It is worth noting that the Stix model has been used to estimate minority ion tail temperatures that are higher than this.[23] However, for the reasons noted above, such estimates are highly uncertain.

As we indicated earlier, in order to compute $\mathrm{Re}(\delta\tilde{W}_k)$ it is necessary to specify *inter alia* the minority ion concentration $\eta\equiv n_h/n_e$, the electron temperature T_e, and the electron density n_e.[6] The minority ion concentration in discharges A and B was rather uncertain: relative to the deuteron density, it may have been as low as 2% or as high as 10%.[4] Here, we set $\eta=0.02$ at all r. We assume electron temperature and density profiles of the form

$$T_e(r)=T_{e0}\left[1-\left(\frac{r}{a}\right)^2\right]^{\nu_{Te}}, \tag{13}$$

$$n_e(r)=n_{e0}\left[1-\left(\frac{r}{a}\right)^2\right]^{\nu_{ne}}. \tag{14}$$

Figure 3 of Ref. 2 depicts $T_e(r)$ at various times during discharge A, and, in particular, during the period immediately preceding the termination of the sawtooth-free period. Fitting Eq. (12) to the observed values of $T_e(r)$ inside the sawtooth inversion radius, we obtain $\nu_{Te}=1.90\pm0.05$. The value of T_{e0} during the sawtooth-free period, as we noted in the Introduction, was approximately 6.4 keV. The electron density profile in discharge A was much flatter than the temperature profile, with $\nu_{ne}\simeq0.7$. The mean electron density along a line passing through the plasma center was approximately 1.5×10^{19} m^{-3} (see Fig. 2 of Ref. 2). Performing the appropriate integral of Eq. (14) with respect to r, we infer from this that $n_{e0}\simeq2.1\times10^{19}$ m^{-3}.

The electron temperature profile also has a bearing on the minority ion parallel temperature, $T_\parallel$. Stix[21] suggested that

$$T_\parallel\simeq3.7T_e(2A^{1/2}Z_{\rm eff})^{2/3}\ \ {\rm keV}, \tag{15}$$

where $Z_{\rm eff}$ is defined in the usual way and A is the minority ion mass number. Setting $T_{e0}=6.4$ keV, $A=1$, and $Z_{\rm eff}=4$,[23] we obtain $T_\parallel(0)\simeq95$ keV. With $T_\perp(0)=140$ keV, this implies that $T_\parallel(0)/T_\perp(0)\simeq0.7$ in discharge A. In this case F_h is only weakly anisotropic at $R=R_0$. Since $T_\perp$ is expected to have a stronger dependence on r than $T_\parallel$ [compare Eq. (13) with Eq. (15)], the value of $T_\parallel/T_\perp$ at finite r is likely to be even higher than 0.7. To model discharge A, we set $T_\parallel/T_\perp$ equal to 0.85 at all r.

Finally, we adopt the following generic representation of the safety factor profile $q(r)$:

$$q(r)=q_0[1+\lambda_q(r/a)^{2\nu}]^{1/\nu}, \tag{16}$$

where $a\simeq1.25$ m and q_0, λ_q, and ν are constants. In choosing appropriate values for these constants, we note from Ref. 2 that q_0 was observed to fall by around 10% during the course of the sawtooth-free period in discharge A, its initial value lying approximately in the range 0.9–1.0. The sawtooth inversion radius r_i was observed to increase from about 0.4 m prior to ICRH stabilization, to around 0.5–0.6 m at the time of the sawtooth collapse which terminated the stable period. If r_i is approximately equal to the radius of the $q=1$ surface r_1, there must have been a steep gradient in q at $r>r_1$, in order to give $q_a\sim5$ throughout the discharge. This suggests that $\nu>1$ is appropriate in Eq. (16). To describe the plasma conditions at the start of the sawtooth-free period, we set $q_0=0.8$, $\lambda_q=41.2$, and $\nu=2$, so that $r_1\simeq0.34a\simeq0.4$ m. To describe the end of the sawtooth-free period, we set $q_0=0.7$, $\lambda_q=149.4$, and $\nu=2.5$, giving $r_1\simeq0.40a\simeq0.50$ m. The parameter set required to evaluate Re($\delta\tilde{W}_k$) is completed by the major radius R_0 and the axial magnetic induction B_0: in discharges A and B, $R_0=3$ m and $B_0=2.2$ T.

B. Toroidal contribution to kink energy

As we noted at the beginning of this section, $\delta\tilde{W}_T$ was shown in Ref. 5 to be a quadratic function of β_p, which depends on the total plasma pressure profile. In Ref. 6 it was noted that the pressure of an ICRF-heated plasma is not a scalar quantity, since the heated ion distribution is anisotropic (cf. Fig. 1). Even when the ICRF power is relatively low (e.g., 4–6 MW), the product $n_hT_\perp$ is typically comparable to, or greater than, the electron pressure n_eT_e. The internal kink stability criteria obtained by Bussac and coworkers in Ref. 5 have been extended by Mikhailovskii[8] to the case of a tokamak plasma in which the pressure is anisotropic but only weakly dependent on poloidal angle θ. Madden and Hastie[9] have obtained hydromagnetic equilibria for tokamaks in which the pressure is both anisotropic and θ dependent. Expanding the perpendicular pressure $p_\perp$ as a Fourier cosine series in θ, Madden and Hastie obtained a generalized second-order equation for the Shafranov shift $\Delta(r)$. The extra terms in this equation, neglected in previous calculations, involve the Fourier coefficient of $\cos2\theta$. In the expression for $\delta\tilde{W}_T$ that was obtained in Ref. 5, the β_p and β_p^2 terms arise from $\Delta'(r_1)\neq0$, and so modifications to the equation for $\Delta(r)$, such as those deduced in Ref. 9, imply that $\delta\tilde{W}_T$ must also be modified. To compute $\delta\tilde{W}_T$, we must therefore determine the θ dependence of $p_\perp$, which is defined in terms of F_h by the expression

$$p_\perp(r,\theta)=\pi\int_{-\infty}^{\infty}dv_\parallel\int_0^\infty m_hv_\perp^3F_h\ dv_\perp. \tag{17}$$

The quantity $p_\perp$ must be evaluated separately for poloidal angles lying inboard and outboard of the magnetic axis. In both cases, we obtain an expression of the form

$$p_\perp(r,\theta)=2Gn_h(T_\parallel T_\perp)^{1/2}\left[1+\mathcal{O}\left(\epsilon\frac{T_\perp}{T_\parallel}\right)\right], \tag{18}$$

where the $\mathcal{O}(\epsilon T_\perp/T_\parallel)$ are θ dependent. The coefficients of $\cos2\theta$, in particular, are of order $\epsilon T_\perp/T_\parallel$. As we noted in the previous section, the ICRF-heated ion distribution is likely to be only weakly anisotropic when the radio-frequency power is low: in such cases $\epsilon T_\perp/T_\parallel\ll1$, and the $\cos2\theta$ term in the Fourier expansion of $p_\perp$ can be neglected. We may then apply the analysis of Mikhailovskii,[8] who obtained a modified form of the result obtained by Bussac and co-workers:[5]

$$\delta\tilde{W}_T=\frac{1}{6}\ \beta_p^c+\delta\tilde{W}_1+\beta_p\ \delta\tilde{W}_2+\beta_p^2\ \delta\tilde{W}_3, \tag{19}$$

where: $\delta\tilde{W}_1$, $\delta\tilde{W}_2$, and $\delta\tilde{W}_3$ depend on the q profile, and must be evaluated numerically; β_p is defined by Eq. (6), with

$$p\equiv p_{\rm bulk}+(p_\parallel+p_\perp)/2, \tag{20}$$

where $p_{\rm bulk}$ is the bulk plasma pressure and

$$p_\parallel=2\pi\int_{-\infty}^{\infty}m_hv_\parallel^2\ dv_\parallel\int_0^\infty v_\perp F_h\ dv_\perp$$

$$\simeq2Gn_h\frac{T_\parallel}{T_\perp}\ (T_\parallel T_\perp)^{1/2} \tag{21}$$

is the minority ion parallel pressure; and β_p^c is defined in the same way as β_p, except that p is replaced by $(p_\parallel + p_\perp + C)/2$, where

$$C = 4\pi m_h \int\int \frac{B}{|v_\parallel|} (\mu B)^2 \frac{\partial F_h}{\partial \mathscr{E}} \, d\mu \, d\mathscr{E}$$

$$\simeq -4 G n_h \frac{T_\perp}{T_\parallel} (T_\parallel T_\perp)^{1/2}. \tag{22}$$

In Eq. (22), $\partial F_h/\partial \mathscr{E}$ is evaluated at constant μ and r. It is clear from Eqs. (18), (21), and (22) that $\beta_p^c = 0$ for a plasma with isotropic pressure, and we then recover the result obtained by Bussac and co-workers.[5] It is clear also that $\beta_p^c < 0$ when, as in the present case, $T_\perp > T_\parallel$. The quantity $\delta\tilde{W}_1$ is always positive and thus stabilizing, whereas $\delta\tilde{W}_2$ and $\delta\tilde{W}_3$ are negative and destabilizing. Expressions for $\delta\tilde{W}_1$, $\delta\tilde{W}_2$, and δW_3 are given in Ref. 5.

It is convenient to split the poloidal beta into bulk plasma ($\beta_p^{\rm bulk}$) and hot minority ion ($\beta_p^{\rm hot}$) components. The latter quantity must be evaluated numerically. The bulk plasma poloidal beta, on the other hand, can be evaluated analytically. If we make the reasonable assumption that the majority ions and electrons have identical density and temperature profiles (except for normalization), and neglect the contribution to the pressure of plasma impurities, it follows from Eqs. (13) and (14) that

$$p_{\rm bulk} = (n_{e0} T_{e0} + n_{i0} T_{i0}) \left(1 - \frac{r^2}{a^2}\right)^{\nu_p}, \tag{23}$$

where T_{i0}, n_{i0} denote central values of the majority ion temperature and density, and $\nu_p = \nu_{ne} + \nu_{Te}$. Writing $p_0 = n_{e0} T_{e0} + n_{i0} T_{i0}$, it is straightforward to show that

$$\beta_p^{\rm bulk} = \frac{2\mu_0 p_0}{\epsilon_1^4 B_0^2} \frac{a^2}{R_0^2} \left\{ \left[1 - \left(1 - \frac{r_1^2}{a^2} \right)^{\nu_p} \right] - \frac{\nu_p}{\nu_p + 1} \left[1 - \left(1 - \frac{r_1^2}{a^2} \right)^{\nu_p + 1} \right] \right\}. \tag{24}$$

Expanding the right-hand side of Eq. (24) in ascending powers of r_1^2/a^2, we obtain an expression that is independent of r_1:

$$\beta_p^{\rm bulk} \simeq \frac{\mu_0 \nu_p p_0}{B_0^2} \frac{R_0^2}{a^2}. \tag{25}$$

The only parameters appearing in $\beta_p^{\rm bulk}$ that we have not already specified are n_{i0} and T_{i0}. Figure 2 of Ref. 2 indicates that $T_{i0} \simeq 5.5$ keV during the sawtooth-free period of discharge A. To deduce a value for n_{i0}, we assume that the main impurity in the plasma is carbon.[23] Setting $Z_{\rm eff} = 4$,[23] $n_{e0} = 2.1 \times 10^{19}$ m^{-3}, and $\eta = 0.02$, we infer that $n_{i0} \simeq 8 \times 10^{18}$ m^{-3}.

C. Shape contribution to kink energy

The shape contribution to $\delta\tilde{W}$ is independent of β_p, and may be evaluated numerically for any specified plasma boundary shape using the analysis presented in Ref. 7. In general, R and Z at the plasma boundary may be expressed, respectively, as Fourier cosine and sine series in the poloidal angle θ. Here, we truncate each series at the second harmonic and write

$$R = R_0 - \Delta(a) + a[(1 - E)\cos\theta + T\cos 2\theta], \tag{26}$$

$$Z = a[(1 + E)\sin\theta - T\sin 2\theta], \tag{27}$$

where E and T are constants representing the elongation and triangularity of the boundary. When E, T, and the q profile have been specified, $\delta\tilde{W}_{\rm shape}$ may be evaluated using Eq. (46) in Ref. 7. The elliptical and triangular distortions of the flux surface cross section increase with r, and so plasma shaping becomes more significant as r_1 rises.

An alternative representation of shaping that is simpler and more commonly used in the tokamak plasma literature is the following:[27]

$$R = R_0 - \Delta(a) + \frac{2a}{1 + \kappa} \cos\tilde{\theta}, \tag{28}$$

$$Z = \frac{2\kappa a}{1 + \kappa} \sin(\tilde{\theta} - \delta\sin\tilde{\theta}), \tag{29}$$

where κ, δ are constants and $\tilde{\theta} \in [0, 2\pi]$ is a parameter that generates the boundary: it is not exactly equivalent to the variable θ used in Eqs. (26)–(27). A simple relation between E and κ may be obtained by requiring the two plasma boundaries to have the same midplane width:

$$E = \frac{\kappa - 1}{\kappa + 1}. \tag{30}$$

The value of T that corresponds most closely to specified values of κ and δ may be obtained graphically, by superimposing plots of Eqs. (26)–(27) and Eqs. (28)–(29). Setting $\kappa = 1.5$, $\delta = 0.2$, $E = 0.2$, and $T = 0.05$, we obtain plasma boundary cross sections that closely resemble those of the JET discharges of interest (see, e.g. Fig. 3 in Ref. 28): they are plotted in Fig. 2, with R and Z normalized to $2a/(1+\kappa)$ and the coordinate system centered on $R = R_0 - \Delta(a)$, $Z = 0$. Equations (28)–(29) are represented by the solid curve, and Eqs. (26)–(27) by the dashed curve. It is clear that the two boundaries coincide almost exactly. Thus, it is appropriate to compute $\delta\tilde{W}_{\rm shape}$ with E and T, respectively, set equal to 0.2 and 0.05.

D. Numerical results

The hot minority ion, toroidal, and shape contributions to $\mathrm{Re}(\delta\tilde{W})$, at the beginning and end of the sawtooth-free period, are listed in Table I. The poloidal beta is sufficiently large that $\delta\tilde{W}_T < 0$ throughout the period in question. A modest rise in $\mathrm{Re}(\delta\tilde{W}_k)$ is accompanied by much larger increases in both $|\delta\tilde{W}_T|$ and $|\delta\tilde{W}_{\rm shape}|$, the result being that $\mathrm{Re}(\delta\tilde{W})$ changes sign, from positive to negative. Thus, the model parameters inferred in the preceding sections are consistent with a scenario in which the ideal internal kink mode becomes unstable at a time corresponding roughly to the end of the sawtooth-free period. Whereas $\beta_p^{\rm bulk}$ remains approximately constant during the sawtooth-free period [cf. Eq. (25)], $\beta_p^{\rm hot}$ and $|\beta_p^c|$ both fall by nearly a factor of 2, due to expansion of the $q \leqslant 1$ volume. As we noted previously, the

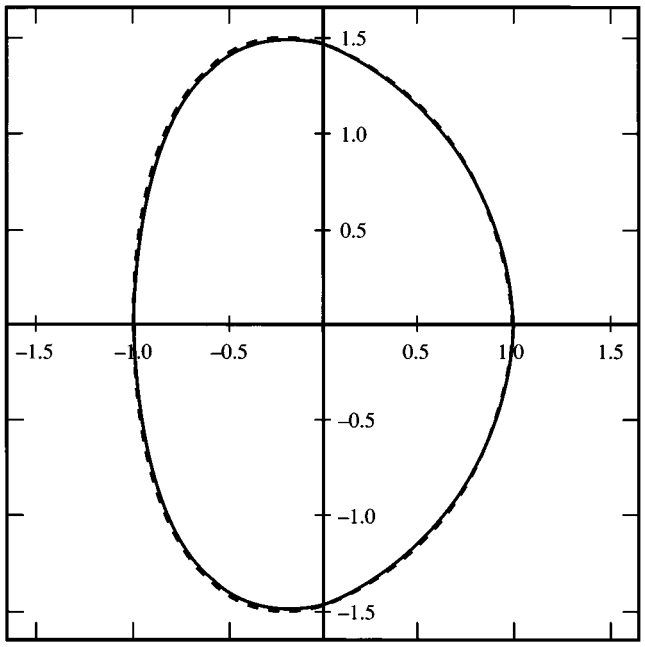

FIG. 2. Solid curve: plasma boundary defined by Eqs. (26) and (27), with $\kappa=1.5$, $\delta=0.2$. Dashed curve: plasma boundary defined by Eqs. (24) and (25), with $E=0.2$, $T=0.05$.

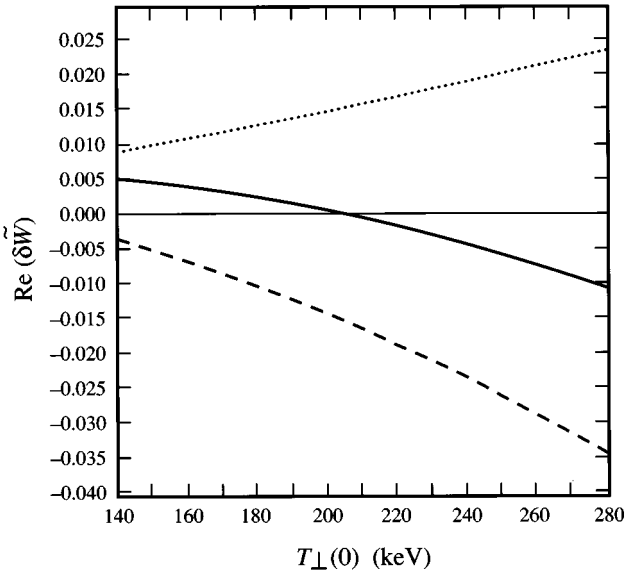

FIG. 3. Solid line: dimensionless kink energy Re$(\delta\tilde{W})$ as a function of $T_\perp(0)$, the perpendicular temperature of heated minority ions at the magnetic axis. Dotted line: trapped minority ion contribution to Re$(\delta\tilde{W})$. Dashed line: toroidal and shape contributions to Re$(\delta\tilde{W})$. The e-folding widths of the ICRF power deposition profile in the vertical and major radial directions are, respectively, $D=20$ cm and $d=15$ cm. The q profile is defined by $q_0=0.8$, $\nu=2$, and $\lambda_q=41.2$. The other parameters are given in the text. A central minority ion temperature of 140 keV corresponds to a total ICRF wave power P_{RF} of around 4 MW (as in the sawtooth-free period of discharge A), while $T_\perp(0)=210$ keV corresponds to $P_{\mathrm{RF}}\simeq 6$ MW (as in discharge B, which exhibited continuous sawtooth behavior).

coefficients of β_p and β_p^2 in Eq. (19) are negative, and so these terms, along with $\beta_p^c/6$, are sources of instability. Despite a drop in the hot minority ion contribution to the toroidal energy, the change in the q profile is such that $|\delta\tilde{W}_T|$ and $|\delta\tilde{W}_{\mathrm{shape}}|$ rise sufficiently rapidly to bring about destabilization. Qualitatively, it is not surprising that the shape term should increase with r_1, since flux surface cross sections become progressively less circular toward the plasma boundary. It should be stressed, however, that $\delta\tilde{W}_{\mathrm{shape}}$ is also very sensitive to the parameter ν: the sharp increase in $|\delta\tilde{W}_{\mathrm{shape}}|$ between the beginning and end of the sawtooth-free period is due largely to a flattening of the q profile at $r<r_1$.

We now evaluate Re$(\delta\tilde{W})$ for a range of values of $T_\perp(0)$, recalling that discharges A and B are assumed to be identical, except for the value of this parameter. In particular, we assume that the two discharges have the same q profiles. Figure 3 shows Re$(\delta\tilde{W})$ (dotted line), $\delta\tilde{W}_T+\delta\tilde{W}_{\mathrm{shape}}$ (dashed line), and Re$(\delta\tilde{W})$ as functions of $T_\perp(0)$. The parallel temperature is held fixed, so that $T_\perp/T_\parallel$ increases linearly with $T_\perp$. Equation (12) indicates that $T_\perp(0)$ should scale with P_{RF}, and, since P_{RF} is about 50% higher in discharge B than it is in discharge A, we estimate that $T_\perp(0)\simeq 210$ keV in discharge B. Again, a relatively modest rise in Re$(\delta\tilde{W}_k)$, is offset by a more rapid increase in $|\delta\tilde{W}_T+\delta\tilde{W}_{\mathrm{shape}}|$, with the result that Re$(\delta\tilde{W})$ becomes negative as the ICRF power is increased. The essential reason for this is that Re$(\delta\tilde{W}_k)$ scales approximately with β_p^{hot}, whereas $\delta\tilde{W}_T$ contains a numerically negative term that scales with $(\beta_p^{\mathrm{hot}})^2$. A sufficiently large increase in minority ion pressure thus has a destabilizing effect. The present authors have predicted a similar phenomenon in ignited plasmas, when alpha particles make a significant contribution to the plasma pressure.[29] If Re$(\delta\tilde{W})<0$ is a sufficient condition for the occurrence of a sawtooth crash, the change in sign of Re$(\delta\tilde{W})$ with increasing $T_\perp(0)$ is wholly consistent with the observation that sawteeth are suppressed in discharge A [$P_{\mathrm{RF}}\simeq 4$ MW; $T_\perp(0)\simeq 140$ keV], but not in discharge B [$P_{\mathrm{RF}}\simeq 6$ MW; $T_\perp(0)\simeq 210$ keV].[2] Our results are also consistent with experimental data published by Bhatnagar and co-workers,[16] which indicate that sawtooth periods in ICRF-heated JET discharges can be maximized by choosing P_{RF} to be in the 3–5 MW range. Values of P_{RF} in this range have been shown to optimize sawtooth stabilization in TFTR.[3] It is important to stress that our calculation of $\delta\tilde{W}_k$ assumes zero orbit widths,[6] and so the mechanism we are proposing for sawtooth destabilization at high ICRF power is distinct from that proposed by Porcelli and co-workers in Ref. 15.

Finally, in Fig. 4 we plot Re$(\delta\tilde{W}_k)$, $\delta\tilde{W}_T+\delta\tilde{W}_{\mathrm{shape}}$, and Re$(\delta\tilde{W})$ as functions of D, the height of the ICRF wave absorption profile. The other parameters are those of discharge A. It is apparent that the overall sign of Re$(\delta\tilde{W})$ is

TABLE I. Safety factor parameters and contributions to dimensionless kink energy at early (second column) and late (third column) stages of the sawtooth-free period in discharge A.

q_0	0.8	0.7
r_1/a	0.34	0.40
q_a	5.2	5.2
Re$(\delta\tilde{W}_k)$	0.0089	0.0098
$\delta\tilde{W}_T$	−0.0015	−0.0046
$\delta\tilde{W}_{\mathrm{shape}}$	−0.0024	−0.0074
Re$(\delta\tilde{W})$	0.0050	−0.0022

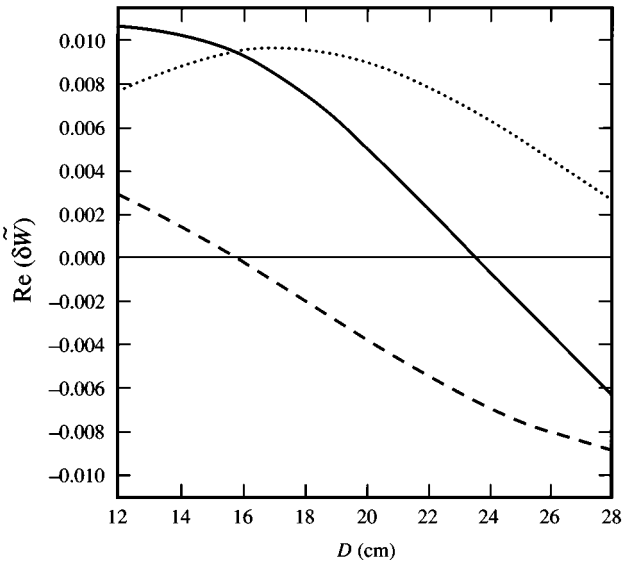

FIG. 4. As Fig. 3, except that $\mathrm{Re}(\delta\tilde{W}_k)$, $\delta\tilde{W}_T+\delta\tilde{W}_{\mathrm{shape}}$, and $\mathrm{Re}(\delta\tilde{W})$ are plotted as functions of D, the height of the ICRF power deposition profile. The value of $T_\perp(0)$ is 140 keV.

crucially dependent on the value of D. While β_p^{hot} and $|\beta_p^c|$ increase monotonically with D, the dependence of $\delta\tilde{W}_k$ on this parameter is more complex. When D is small, minority ions are only heated close to the plasma center, and a negligible proportion of such ions are trapped. When D is large, on the other hand, F_h has a flat radial profile. In both limits, it is clear from Eq. (7) that $\delta\tilde{W}_k\rightarrow 0$. In the case of discharge A, the value of D that gives a maximum $\delta\tilde{W}_k$ is around 18 cm. Since the value of D is determined essentially by wave focusing, the conclusion to be drawn from Fig. 4 is that stabilization can be achieved most easily by using strongly focused ICRF waves.

In Ref. 4 it was noted that the imaginary part of $\delta\tilde{W}_k$ is associated with a finite mode frequency. In every case considered above, we find that the value of $\mathrm{Im}(\delta\tilde{W}_k)$ corresponds to a real ω that is much smaller than the typical precessional drift frequency of the heated minority ions: this is a requirement for the analysis presented in Ref. 6 to be self-consistent.

IV. DISCUSSION

Using a realistic model of ICRF power deposition, we have shown that the best-fit plasma parameters of an ICRF-heated discharge in JET are consistent with a scenario in which the $m=1$ internal kink energy δW changes sign (from positive to negative) at approximately the same time as a sawtooth crash that terminated a period of negligible MHD activity. We have shown also that an increase in the coupled ICRF power may bring about an overall decrease in δW, leading to greater instability, as observed. From this we infer that the MHD energy principle, generalized to include kinetic effects associated with trapped energetic ions, is a useful tool for predicting the occurrence of sawtooth oscillations.

We have so far neglected the effects of finite resistivity, which tends to lower the threshold for instability. Taking into account the effects of diamagnetic rotation, Porcelli and Migliuolo[30] obtained the following criterion for instability of the resistive $m=1$ internal kink mode in a high-temperature tokamak plasma:

$$\mathrm{Re}(\delta\tilde{W})\lesssim\delta\tilde{W}_{\mathrm{crit}}\equiv\frac{s_1^2}{3\epsilon_1^2(\tau_\eta\hat{\omega}_{*e})^{1/2}},\tag{31}$$

where $s_1=s(r_1)=r_1q'(r_1)$; $\tau_\eta=\mu_0r_1^2/\eta_e$, where η_e is resistivity; and $\hat{\omega}_{*\mathrm{e}}$, the electron diamagnetic frequency, is related to the electron temperature and density gradients. All quantities on the right-hand side of Eq. (31) are evaluated at $r=r_1$: using the parameter values adopted for discharge A and the usual Spitzer expression for η_e, we find that $\delta\tilde{W}_{\mathrm{crit}}$ is comparable in magnitude to the values obtained for $\mathrm{Re}(\delta\tilde{W})$ in Table I and Figs. 3–4, which suggests that resistive effects may indeed play an important role in determining sawtooth stability. However, it is noted in Ref. 30 that Eq. (31) is only valid if

$$\frac{\hat{\omega}_{*e}}{\omega_{\mathrm{A}}}>\left(\frac{\eta_e}{\mu_0r_1^2\omega_{\mathrm{A}}}\right)^{1/3},\tag{32}$$

where $\omega_{\mathrm{A}}=s_1v_{\mathrm{A}}/\sqrt{3}R_0$, v_{A} being the Alfvén speed. Equation (32) becomes progressively less well satisfied during the course of the sawtooth-free period in discharge A. In any case, comparisons between Eq. (31) and experimental data must be treated with caution, since $\delta\tilde{W}_{\mathrm{crit}}$ is a sensitive function of s_1, accurate values of which are difficult to obtain.

We have assumed in this paper that $\mathrm{Re}(\delta\tilde{W})<0$ is a sufficient condition for the occurrence of a sawtooth crash. It is appropriate at this stage to compare, as far as possible, the sawtooth stability criterion obtained by Zakharov and co-workers in Ref. 31. The negative value of $\mathrm{Re}(\delta\tilde{W})$ that we compute for the end of the sawtooth-free period in discharge A (see Table I) implies an ideal $m=1$ kink mode layer width λ_h whose modulus is smaller than both the bulk ion Larmor radius ρ_i and the collisionless skin depth d_e. Zakharov and co-workers proposed a sawtooth model involving collisionless reconnection, and obtained a criterion for instability of the $m=1$ reconnection mode that is applicable in this régime, and that was later applied by Levinton and co-workers[19] to TFTR:

$$s_1\gtrsim 1.4\,\frac{\beta^{2/3}}{Z_{\mathrm{eff}}^{1/6}}\left(\frac{|n_e'|R_0}{n_e}\right)^{2/3}\left(\frac{|p'|R_0}{p}\right)^{1/3},\tag{33}$$

where β is the toroidal plasma beta, p is plasma pressure (assumed to be isotropic), primes denote radial derivatives, all quantities are evaluated at $r=r_1$ [as in Eq. (31)], and we have assumed that the majority ions are deuterons. Equation (33) appears to provide a reliable means of predicting the occurrence of sawteeth in TFTR when $\mathrm{Re}(\delta\tilde{W})$ lies close to zero (see Fig. 3 in Ref. 19). For comparison with our approach, we set $p=p_{\mathrm{bulk}}+(p_\parallel+p_\perp)/2$ [cf. Eq. (20)] in Eq. (33), and, adopting the parameters used in Table I to model the end of the sawtooth-free period in discharge A, find that Eq. (33) is satisfied. However, this conclusion depends on an assumed value of s_1, which, as we have noted above, is

difficult to measure in JET. Moreover, it is not clear how Eq. (33) should be modified when, as in the present case, the plasma pressure contains a significant contribution from ICRF-heated ions, and is thus anisotropic. The sawtooth criteria obtained by Zakharov and co-workers are that $|\lambda_h|$ be smaller than both ρ_i and d_e, and that Eq. (33) be satisfied: the parameter set used in Table I to model the end of the sawtooth-free period in discharge A satisfies these criteria (subject to the above caveats) and, according to the analysis of Zakharov and co-workers, is sawtooth unstable. For the parameter set used in Table I to model the beginning of the sawtooth-free period, we find that $|\lambda_h| > d_e$, in which case Eq. (33) is not applicable and therefore cannot be used to predict the occurrence of a sawtooth crash.

Following the suggestion by Levinton and co-workers[19] that $\delta\tilde{W}$ was strongly negative in sawtooth-free TFTR discharges, Rogers and Zakharov[20] used a two-fluid MHD model, with isotropic plasma pressure, to demonstrate numerically and analytically that a linearly unstable $m=1$ mode can saturate at a very low level, under certain conditions. These conditions are: that both ρ_i and d_e be much smaller than $|\lambda_h|$; and that ω_{*i} and $|\hat{\omega}_{*e}|$ exceed a certain fraction of ω_A. In the case of the parameter sets used to generate Table I and Figs. 3–4, the inequality $|\lambda_h| \gg \rho_i$ is never satisfied, and the ratios ω_{*i}/ω_A and $|\hat{\omega}_{*e}|/\omega_A$ are about an order of magnitude smaller than the values assumed by Rogers and Zakharov in their MHD simulation. Thus, the conclusions reached by Rogers and Zakharov regarding nonlinear saturation of the $m=1$ apply to a régime that differs from that of the JET discharges considered here.

Although the exact conditions required for instability of the $m=1$ kink mode are thus somewhat uncertain, it is clear that sawtooth suppression is associated with strongly positive values of $\mathrm{Re}(\delta\tilde{W})$. It is thus logical to search for experimentally accessible parameter regimes in which the condition $\mathrm{Re}(\delta\tilde{W}) > 0$ can be maintained for as long as possible. We have noted that an increase in P_{RF} can be destabilizing. However, if the ICRF power level is very low, $\mathrm{Re}(\delta\tilde{W}_k) \ll |\delta\tilde{W}_T + \delta\tilde{W}_{\mathrm{shape}}|$, and instability will then occur whenever β_p lies above a threshold value, which, for the equilibria used to compute Table I and Figs. 3–4, lies in the range 0.08–0.13. Phillips and co-workers[3] have noted the existence of a minimum P_{RF} required to achieve sawtooth stabilization in TFTR. In ICRH experiments carried out on both JET[2,16,32] and TFTR[3] with low minority ion concentration ($\eta < 0.1$), the optimum value of P_{RF} has been found to be around 4 MW.

Clearly, resistivity η is also a key parameter for sawtooth stabilization. In this context, we note that the β_p^c term in $\delta\tilde{W}_T$ is strongly destabilizing if $p_\perp \gg p_\parallel$ [see Eqs. (18), (21), and (22)]. For a fixed value of P_c, the Stix model [Eq. (12)] indicates that an increase in η should be accompanied by a reduction in $T_\perp$, and hence a (stabilizing) reduction in $|\beta_p^c|$. However, the fractional wave power P_c/P_{RF} absorbed by minority ions is itself a sensitive function of η, and so an increase in the latter may not bring about the desired stabilization. Indeed, experiments on JET with 5 MW of ICRH indicate a reduction in the sawtooth period as η is raised from 0.16 to 0.43.[32] This may simply reflect a reduction in P_c/P_{RF}: sawtooth stability can be restored at high values of η by increasing P_{RF} from 5 to 6.5 MW.[32]

According to the results shown in Fig. 4, stability can be enhanced by reducing the height of the ICRF power deposition profile, D. In the case of JET, it is not clear that experimental conditions can be achieved in which D is significantly smaller than the 20 cm used to compute Table I and Fig. 3. In general, however, stabilization of sawtooth oscillations is most likely to be achieved if the ICRF waves are strongly focused.

It should be stressed that the model described in this paper is restricted to parameter régimes in which the heated minority ions are only weakly anisotropic ($\epsilon T_\perp/T_\parallel \ll 1$) and have thin banana orbit widths ($\ll r_1$). For a fixed value of η, the Stix model indicates that $T_\perp$ increases linearly with P_{RF} [see Eq. (12)]. When $\eta \sim 0.02$–0.04 and $P_{RF} \sim 10$–15 MW, as in the high-power ICRH experiments described in Ref. 23, F_h is likely to be highly anisotropic, and the orbit widths of trapped ions may be comparable to r_1.[15] The results presented in Ref. 23 indicate that sawtooth stabilization is possible at much higher values of P_{RF} than those used in the experiments described by Campbell and co-workers in Ref. 2, and by Phillips and co-workers in Ref. 3. For this reason, it is difficult to extrapolate the results of our analysis to the parameter régime of a prototype fusion reactor, such as the proposed International Thermonuclear Experimental Reactor (ITER).[33] However, although our theory would need to be modified to describe auxiliary heating in a machine such as ITER, the destabilizing contribution of heated minority ions to the Shafranov shift of magnetic flux surfaces implies that sawtooth activity will always occur when P_{RF} is sufficiently high.

ACKNOWLEDGMENTS

Figure 1(a) has been reproduced from Ref. 22, with permission from the publisher [the International Atomic Energy Agency (IAEA)] and two of the authors (R. W. Harvey and S. C. Chiu) of that paper. Helpful discussions with D. Campbell, C. Gimblett, A. Gondhalekar, C. Lashmore-Davies, D. Start, and T. Todd are gratefully acknowledged.

This work was funded jointly by the United Kingdom Department of Trade and Industry and Euratom.

[1] S. von Goeler, W. Stodiek, and N. Sauthoff, Phys. Rev. Lett. **33**, 1201 (1974).
[2] D. J. Campbell, D. F. H. Start, J. A. Wesson, C. V. Bartlett, V. P. Bhatnagar, M. Bures, J. G. Cordey, G. A. Cottrell, P. A. Dupperex, A. W. Edwards, C. D. Challis, C. Gormezano, C. W. Gowers, R. S. Granetz, H. Hamnen, T. Hellsten, J. Jacquinot, E. Lazzaro, P. J. Lomas, N. Lopes Cardozo, P. Mantica, J. A. Snipes, D. Stork, P. E. Stott, P. R. Thomas, E. Thompson, K. Thomsen, and G. Tonetti, Phys. Rev. Lett. **60**, 2148 (1988).
[3] C. K. Phillips, J. Hosea, E. Marmar, M. W. Phillips, J. Snipes, J. Stevens, J. Terry, J. R. Wilson, M. Bell, M. Bitter, R. Boivin, C. Bush, C. Z. Cheng, D. Darrow, E. Fredickson, R. Goldfinger, G. W. Hammett, K. Hill, D. Hoffman, W. Houlberg, H. Hsuan, M. Hughes, D. Jassby, D. McCune, K. McGuire, Y. Nagayama, D. K. Owens, H. Park, A. Ramsey, G. Schilling, J. Schivell, D. N. Smithe, B. Stratton, E. Synakowski, G. Taylor, H. Towner, R. White, S. Zweben, and the TFTR Group, Phys. Fluids B **4**, 2155 (1992).
[4] D. J. Campbell (private communication, 1995).
[5] M. Bussac, R. Pellat, D. Edery, and J. L. Soulé, Phys. Rev. Lett. **35**, 1638 (1975).

[6]R. O. Dendy, R. J. Hastie, K. G. McClements, and T. J. Martin, Phys. Plasmas **2**, 1623 (1995).
[7]D. Edery, G. Laval, R. Pellat, and J. L. Soulé, Phys. Fluids **19**, 260 (1976).
[8]A. B. Mikhailovskii, Sov. J. Plasma Phys. **9**, 190 (1983).
[9]N. A. Madden and R. J. Hastie, Nucl. Fusion **34**, 519 (1994).
[10]F. Porcelli, D. J. Campbell, W. D. Diachenko, L.-G. Eriksson, J. Jacquinot, L. S. Levin, D. F. H. Start, and A. Taroni, in *Proceedings of the 17th EPS Conference on Controlled Fusion and Plasma Heating*, Amsterdam, Netherlands, 1990, edited by G. Briffod, A. Nijsen-Vis, and F. C. Schüller (European Physical Society, Petit-Lancy, Switzerland, 1990), Part I, Vol. 14B, p. 327.
[11]F. Pegoraro, F. Porcelli, B. Coppi, P. Detragiache, and S. Migliuolo, in *Plasma Physics and Controlled Nuclear Fusion Research 1988* (International Atomic Energy Agency, Vienna, 1989), Vol. 2, p. 243.
[12]B. Coppi, P. Detragiache, S. Migliuolo, F. Pegoraro, and F. Porcelli, Phys. Rev. Lett. **63**, 2733 (1989).
[13]C. Z. Cheng, Phys. Fluids B **2**, 1427 (1990).
[14]M. Zabiégo, X. Garbet, A. Bécoulet, F. Nguyen, and B. Saoutic, Nucl. Fusion **34**, 1489 (1994).
[15]F. Porcelli, R. Stankiewicz, H. L. Berk, and Y. Z. Zhang, Phys. Fluids B **4**, 3017 (1992).
[16]V. P. Bhatnagar, D. F. H. Start, J. Jacquinot, F. Chaland, A. Cherubini, and F. Porcelli, Nucl. Fusion **34**, 1579 (1994).
[17]R. B. White, P. H. Rutherford, P. Colestock, and M. N. Bussac, Phys. Rev. Lett. **60**, 2038 (1988).
[18]R. B. White, M. N. Bussac, and F. Romanelli, Phys. Rev. Lett. **62**, 539 (1989).
[19]F. M. Levinton, L. Zakharov, S. H. Batha, J. Manickam, and M. C. Zarnstorff, Phys. Rev. Lett. **72**, 2895 (1994).
[20]B. Rogers and L. Zakharov, Phys. Plasmas **2**, 3420 (1995).
[21]T. H. Stix, Nucl. Fusion **15**, 737 (1975).
[22]R. W. Harvey, M. G. McCoy, G. D. Kerbel, and S. C. Chiu, Nucl. Fusion **26**, 43 (1986).
[23]D. A. Boyd, D. J. Campbell, J. G. Cordey, W. G. F. Core, J. P. Christiansen, G. A. Cottrell, L.-G. Eriksson, T. Hellsten, J. J. Jacquinot, O. N. Jarvis, S. E. Kissel, C. Lowrey, P. Nielsen, G. Sadler, D. F. H. Start, P. R. Thomas, P. Van Belle, and J. A. Wesson, Nucl. Fusion **29**, 593 (1989).
[24]G. Sadler, O. N. Jarvis, P. van Belle, and J. M. Adams, in *Proceedings of the 15th EPS Conference on Controlled Fusion and Plasma Heating*, Dubrovnik, Yugoslavia, 1988, edited by S. Pešić and J. Jacquinot (European Physical Society, Petit-Lancy, Switzerland, 1988), Part I, Vol. 12B, p. 131.
[25]F. Tibone, M. P. Evrard, V. Bhatnagar, J. G. Cordey, W. Core, P. A. Dupperex, L.-G. Eriksson, J. C. M. de Haas, H. Hamnen, T. Hellsten, J. Jacquinot, S. Knowlton, R. Koch, H. Lean, F. Rimini, D. Roberts, D. F. H. Start, P. R. Thomas, K. Thomsen, and D. van Eester, in Ref. 24, Part II, Vol. 12B, p. 709.
[26]A. A. Korotkov and A. Gondhalekar, in *Proceedings of the 21st EPS Conference on Controlled Fusion and Plasma Physics*, Montpellier, France, 1994, edited by E. Joffrin, P. Platz, and P. E. Stott (European Physical Society, Petit-Lancy, Switzerland, 1994), Part I, Vol. 18B, p. 266; A. A. Korotkov and A. Gondhalekar, ''Impurity induced neutralization of MeV energy protons in JET plasmas,'' submitted to Nucl. Fusion.
[27]L. C. Bernard, F. J. Helton, R. W. Moore, and T. N. Todd, Nucl. Fusion **23**, 1475 (1983).
[28]The JET Team, in Ref. 11, Vol. 1, p. 41.
[29]K. G. McClements, R. O. Dendy, C. G. Gimblett, R. J. Hastie, and T. J. Martin, Nucl. Fusion **35**, 1761 (1995).
[30]F. Porcelli and S. Migliuolo, Phys. Fluids **29**, 1741 (1986).
[31]L. Zakharov, B. Rogers, and S. Migliuolo, Phys. Fluids B **5**, 2498 (1993).
[32]D. F. H. Start, V. P. Bhatnagar, G. Bosia, M. Bures, D. Campbell, G. A. Cottrell, M. Cox, H. P. L. DeEsch, A. Edwards, L.-G. Eriksson, C. Gormezano, J. Jacquinot, P. Lomas, F. P. Marcus, M. R. O'Brien, F. Porcelli, F. Rimini, D. Stork, A. Tanga, B. Tubbing, C. D. Warrick, and J. Wesson, in *Proceedings of the 1992 International Conference on Plasma Physics*, Innsbruck, Austria, 1992, edited by W. Freysinger, K. Lackner, R. Schrittwieser, and W. Lindinger (European Physical Society, Petit-Lancy, Switzerland, 1992), Part II, Vol. 16C, p. 897.
[33]ITER-JCT and Home Teams, Plasma Phys. Controlled Fusion **37**, A19 (1995).